Improved Metal Object Detection Circuits for Wireless Charging System of Electric Vehicles

Sunhee Kim[1*]
[1] Department of System Semiconductor Engineering, Sangmyung University
Cheonan-si, Chungcheongnam-do, Republic of Korea
[e-mail: happyshkim@smu.ac.kr]
[*]Corresponding author: Sunhee Kim

Received May 11, 2023; revised July 4, 2023; accepted July 16, 2023; published August 31, 2023

Abstract

As the supply of electric vehicles increases, research on wireless charging methods for convenience has been increasing. Because the electric vehicle wireless transmission device is installed on the ground and the electric vehicle battery is installed on the floor of the vehicle, the transmission and reception antennas are approximately 15–30 cm away, and thus strong magnetic fields are exposed during wireless charging. When a metallic foreign object is placed in the magnetic field area, an eddy current is induced to the metallic foreign object, and heat is generated, creating danger of fire and burns. Therefore, this study proposes a method to detect metallic foreign objects in the magnetic field area of a wireless electric vehicle charging system. An active detection-only coil array was used, and an LC resonance circuit was constructed for the frequency of the supply power signal. When a metallic foreign object is inserted into the charging zone, the characteristics of the resonance circuit are broken, and the magnitude and phase of the voltage signal at both ends of the capacitor are changed. It was confirmed that the proposed method has about 1.5 times more change than the method of comparing the voltage magnitude at one node.

Keywords: Electric vehicle, coil array, metal object detection, resonance circuit, wireless charging.

This research was funded by a 2021 Research Grant from Sangmyung University.

http://doi.org/10.3837/tiis.2023.08.014 **ISSN : 1976-7277**

1. Introduction

With the increase in demand for electric vehicles, research on wireless charging systems for electric vehicle batteries has been increasing to improve the convenience of charging these batteries [1-5]. In general, as shown in **Fig. 1**, the power receiving module of a wireless charging system for an electric vehicle battery is installed on the floor of the electric vehicle, and the power transmission module is installed on the ground [6-8]. When an electric vehicle is parked over the power transmission module, power transmission and reception may be performed through wireless communication between the power transmitting and receiving modules. An electric vehicle battery charging system transmits and receives power by a magnetic induction method or a magnetic resonance method using transmitting and receiving coils. Given that 3.7–22 kW of power must be supplied and the transmission and reception coils are approximately 15–30 cm apart, problems such as alignment between coils, shielding, and foreign objects have been studied [9-11].

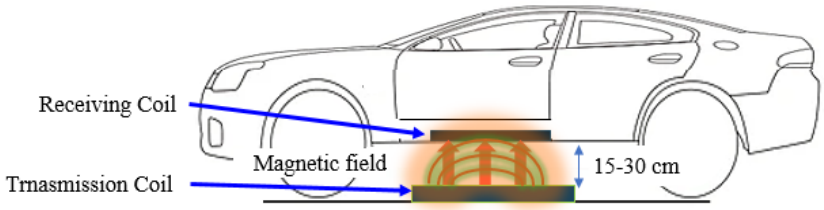

Fig. 1. Position of the transmission and reception coils in an electric vehicle wireless charging system.

During wireless charging of the electric vehicle battery, living objects may enter under the floor of the vehicle, or a metallic foreign object may be inserted between the power transmitting and receiving coils. The strong magnetic field is life-threatening, and living objects can be burnt [12-14]. In the case of a metallic foreign object, an eddy current is induced in the metallic foreign object due to the magnetic field generated by the wireless power transfer. Because a new magnetic field is formed by this eddy current, it affects the power transmitting and receiving coils. The power transmission/reception efficiency is lowered, and the transmitting and receiving modules may be damaged. In addition, fire may occur due to overheating of the metallic foreign object. Therefore, in an electric vehicle battery wireless charging system, it is necessary to be able to detect metallic foreign objects placed between the power transmitting and receiving coils [12-14]. Industry standardization organizations, such as the Wireless Power Consortium (WPC) and SAE International (Society of Automotive Engineers), have issued standards to be complied with. However, the SAE J2954 Standard “Wireless Power Transfer for Light-Duty Plug-in/Electric Vehicles and Alignment Methodology” only includes a standard for test methods for a system that detects metallic foreign objects, but does not specify detection methods [11]. Therefore, various metallic foreign object detection methods have been proposed by different research groups.

Methods for detecting metallic foreign objects can be divided into technologies that use electrical properties and technologies that use non-electric properties [15, 16]. A relatively intuitive detection method is use of non-electrical properties, including pressure or weight sensors, image processing, and deep learning algorithms. In particular, when using image cameras, thermal cameras, and radar sensors, images of the electric vehicle wireless charging system environment can be obtained and analyzed in real–time to classify not only metallic foreign objects but also living objects [17, 18]. However, these methods must be installed

separately outside the wireless power transmission system and are relatively expensive.

The detection method based on electrical properties measures voltage/current and phase changes caused by metallic foreign objects [19]. Because the power transmission coil of the electric vehicle battery charging system is installed on the ground, the metallic foreign object is placed on a high-power transmission coil. When a magnetic field is generated in the transmission coil for power transmission, an eddy current is induced in the metallic foreign object, forming a magnetic field that interferes with the current flow in the power transmission coil. Therefore, metallic foreign objects are detected by monitoring changes such as the current in the transmission coil, reception power strength at the receiving end, and transmission and reception efficiency. However, because metal foreign objects of small size, such as nails, coins, and keys, have smaller impedance than the transmitting and receiving coils, the voltage or current change in the transmission and reception coils created by these metal foreign objects is insignificant.

To detect changes in electrical properties due to metallic foreign objects, a detection-only coil smaller than the transmission coil is used [20, 21]. The detection-only coil is placed above the transmitting module, that is, between the transmitting and receiving coils. Because the metal foreign objects must be detected for the entire section where the magnetic field is formed by the power transmission coil, several detection-only coils are arranged like an array. Detection-only coil methods can be divided into active and passive [14]. Active and passive methods are classified according to whether power is directly connected to the coil.

In general, coils and capacitors are used to detect metal and living foreign objects, respectively. The voltage/current/phase change detection circuits of the two systems may be the same, but the sensing circuits are different. Therefore, in this paper, it is limited to detecting metal foreign objects.

In this paper, we propose a circuit structure for detecting metallic foreign objects in an electric vehicle battery charging system using an active detection-only coil. In the next section, passive and active methods are explained, and a circuit for detecting metallic foreign objects using the active method is proposed. After summarizing the experimental results of the fabricated coil array and circuits, we conclude the paper.

2. Detection coil array and detection circuits

2.1 Conventional methods using a detection-only coil

The passive detection-only coil method uses a detection-only coil in addition to power transmitting and receiving coils, and does not supply separate power to the detection circuit including the passive detection coil. Instead, a magnetic field is induced in the detection coil by the magnetic field during wireless power transmission. An eddy current flows in the detection coil owing to the induced magnetic field, and as a result, current flows in the detection circuit.

In the case of the passive detection-only coil method, the coils located in symmetric positions with respect to the power transmission magnetic field are configured as one set [20-23]. As shown in **Fig. 2a**, a set of coils is connected, and during power transfer, the directions of the magnetic fields induced in the coils are opposite to each other. The currents induced in the coils cancel each other out so that the current is approximately zero [22]. Alternatively, as shown in **Fig. 2b**, the set of coils is not directly connected but placed symmetrically. Therefore, the amount of induced current is the same, and the current difference between the two coils is approximately zero [20]. When a metal object (MO) is placed on one of the coils, the balance

of the magnetic field induced in the two coils is broken and the amount of current changes. Therefore, when a change in the current or voltage of the detection circuit is sensed, it can be detected that an MO has been inserted.

(a) (b)

Fig. 2. Layout of passive detection-only coil sets.
(a) a balanced coil set [22] and (b) symmetric coil sets [20]

The active detection-only coil method supplies separate power to the coil and detection circuit. Therefore, it is possible to detect MOs even when wireless power is not transmitted. Similar to the passive type, one coil is made small to detect relatively small MOs, but it is composed of an array to detect MOs in the entire area of wireless power transmission.

The MO detection circuit measures and compares the magnitude or phase of the voltage/current. As shown in **Fig. 3**, when an AC current of $\omega = 2\pi f$ flows through the detection coil, the impedance of the detection coil is $Z_D = j\omega L_D$. Then, an MO is placed on the detection coil, and the impedance on the detection coil side changes as much as (1) owing to the mutual inductance M between the detection coil and the MO [24].

$$\Delta Z = \left(\frac{\omega^2 M^2}{Z_M Z_M^*}\right)\left\{R_M - j\left(\omega L_M - \frac{1}{\omega C_M}\right)\right\} \tag{1}$$

where Z_M is the impedance of the MO, and R_M, L_M, and C_M represent the resistance, inductance, and capacitance components of the MO, respectively.

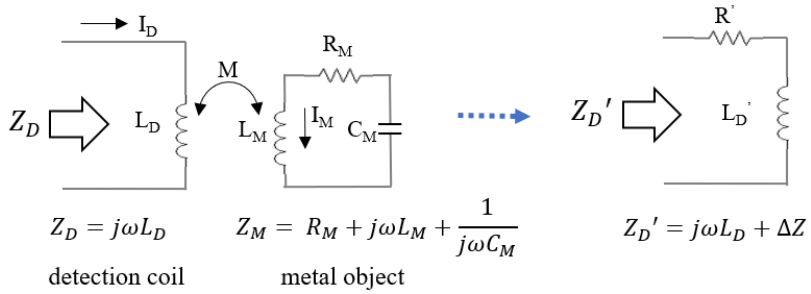

Fig. 3. Equivalent circuits of the detection coil, a metal object, and changed impedance due to mutual inductance

The capacitor is connected to the detection coil to maximize the voltage/current change according to the change in reactance. The capacitor is selected to resonate with respect to the frequency of the power supplied to the active detection coil, thereby composing an LC resonance circuit. When there is no MO, the resonance circuit is tuned to the supply signal, and when an MO is inserted, the resonance is broken by a reactance change. Then, a change occurs in the magnitude and phase of the voltage or current. In [25], the magnitude of the voltage was measured after composing the LC parallel resonance circuit. In [24] and [26], the

magnitude difference and phase difference of a voltage were compared using a series resonance circuit, respectively.

The power transmission/reception system and the active detection-only coil system are configured as shown in **Fig. 4**. The power transmission system consists of an AC-DC converter, a DC-AC inverter, impedance compensation circuits and a transmission coil. The power receiving system consists of a receiving coil, a rectifier, a DC-DC converter, a charger and a battery. The detection system consists of an AC generator/controller, detection circuits and a detection coil. The transmission coil is shielded with aluminum and ferrite to increase the coupling coefficient between the transmitting and receiving coils. There is a detection coil over the transmission coil, and Teflon is placed between the detection and the transmission coil. The receiving coil is shielded with aluminum and ferrite like the transmission coil. Metal foreign objects are placed on top of the detection coil.

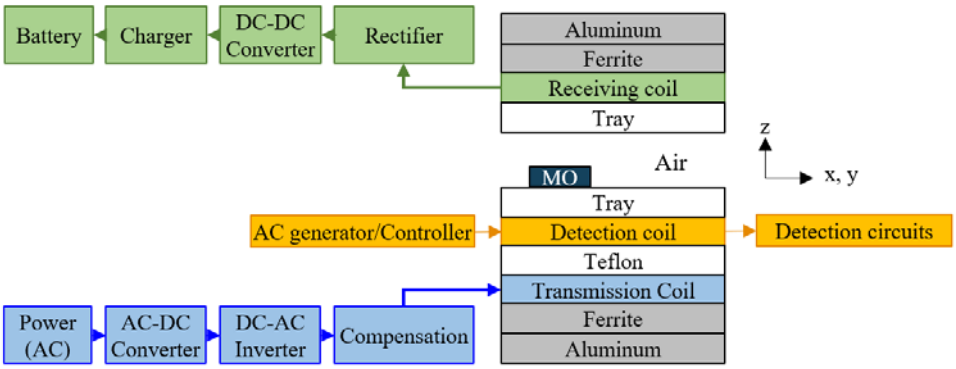

Fig. 4. Diagram of a power transmission/reception system and an active detection-only coil system

2.2 Proposed detection coil array and detection circuits

2.2.1 Detection coil array

The metal object detection(MOD) coil array was designed as shown in **Fig. 5**. Each coil was designed with a spiral coil of 50 mm × 50 mm. In consideration of the size of the power transmission coil of the electric vehicle wireless charging system, the MOD coil was configured in a 10 × 14 array.

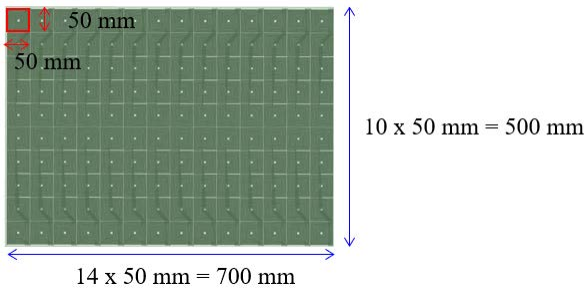

Fig. 5. Designed MOD coil array.

The power supply frequency of the active MOD coil was 1 MHz, which is different from the wireless power transmission frequency of 85 kHz specified in the SAE J2954 Standard

[11]. After designing the MOD coil array with ANSYS Q3D, the inductance of individual FOD coils according to frequency was analyzed. **Fig. 6** shows the analysis results for 10 coils. Although the inductance values differed slightly depending on the location, each port had a value of 13.19 to 13.41 μH at a frequency of 1 MHz. When a metal piece with the size of a Korean 100 won coin (2.4 cm in diameter) is modeled and placed on the coil, the inductance of the coil decreases to approximately 8.5μH.

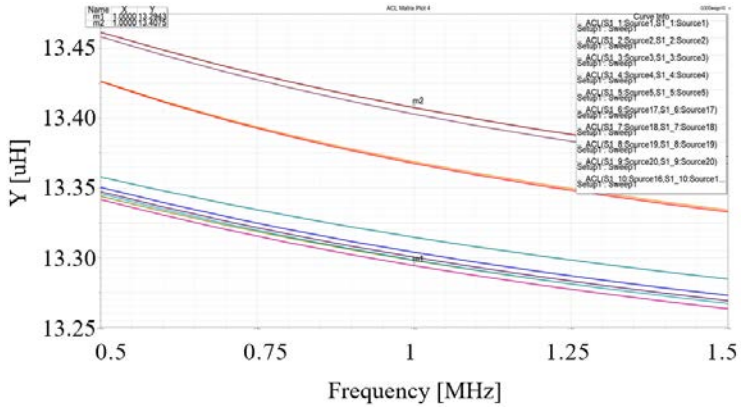

Fig. 6. Inductance analysis of ten detection coils.

2.2.2 Detection circuits

Existing circuits compare the voltage magnitude and phase difference at a specific node of an LC resonance circuit. This study compares the voltage magnitude and phase difference across the resonant capacitor. In the proposed detection circuit as shown in **Fig. 7**, L is the inductance of the detection coil, and C is the capacitance for composing the LC resonance circuit for the frequency of the V_{AC}. Here, R_N, C_N, and L_N refer to the pair of detection coils and resonant circuits. For both nodes of capacitor C_N, the voltage at the node connected to R_N is V_{Na}, and the voltage at the node connected to L_N is V_{Nb}.

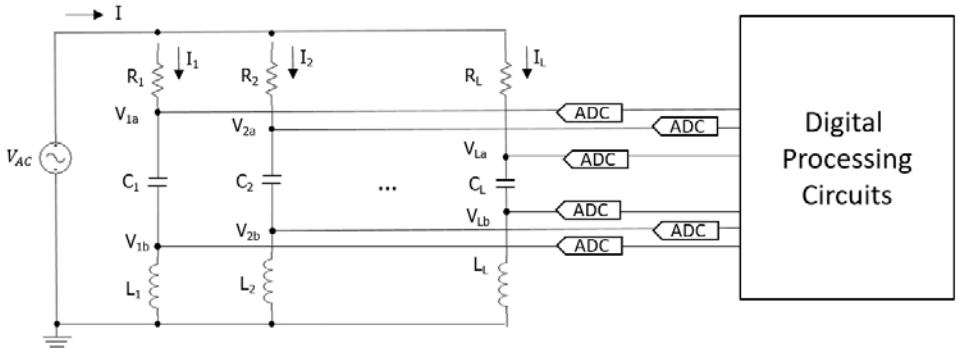

Fig. 7. Proposed detection circuits.

The phasor diagrams as shown in **Fig. 8** represents the total impedance, starting from the ground to L, C, and R. As shown in **Fig. 8.a**, when there is no MO, the magnitudes of the impedance of L_1 and C_1 are the same and the phases are 180° apart, so the total impedance Z = R. Looking at the impedance value at both ends of the capacitor, it is jwL at node b and jwL – j(1/(wC)) = 0 at node a. Therefore, the voltage at V_b is 90° ahead of the supply voltage and

has a constant magnitude ratio, and the voltage at V_a becomes zero. When an MO is placed on the detection coil, the magnitude and phase of the impedance at nodes a and b change, as shown in **Fig. 8.b**. At node b, the magnitude of the impedance decreases such that at node a, the magnitude of the impedance is no longer zero. The phase difference between nodes a and b is approximately 180°.

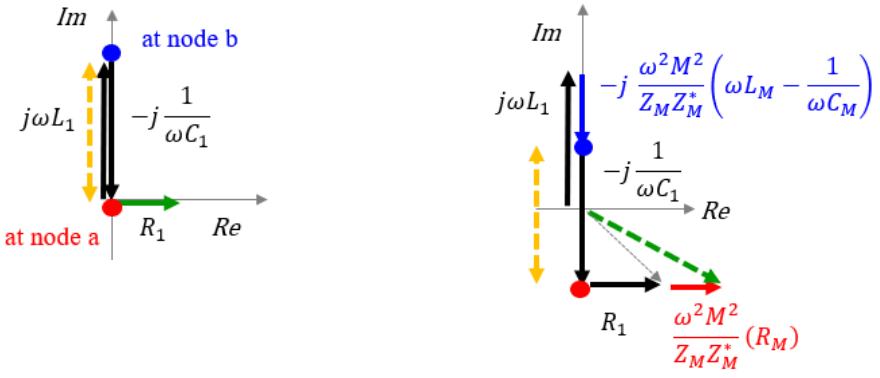

(a) (b)

Fig. 8. Phasor diagrams, (a) without and (b) with metal object (MO).

Fig. 9 shows the PSpice simulation results. In **Fig. 9**, number 1 (green) is the supply voltage signal from the V_{AC}. The frequency of the supply voltage is 1 MHz, which is higher than the power transmission frequency of 75 kHz. L was set to 13 μH according to the ANSYS Q3D analysis results of the coil model, and C was set to 2 nF for LC resonance. R is 200Ω. In the simulation results, numbers 2 and 3 (the solid purple and solid red lines) are the voltages at nodes b and a, respectively, in the absence of an MO. It can be observed that the magnitude of the voltage at node a is almost 0 V, and at node b the voltage is approximately 90° ahead of the supply voltage and the voltage is approximately 0.41 V_{pp}.

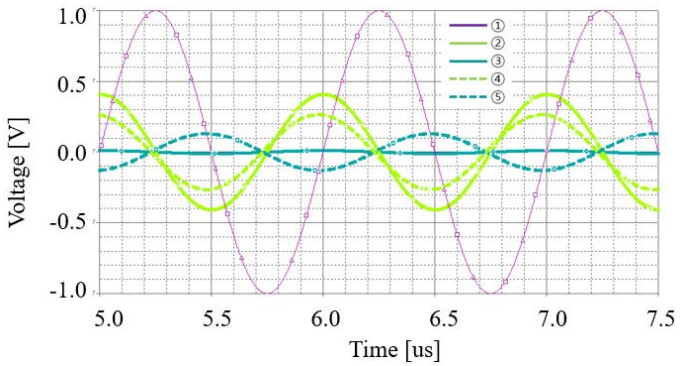

Fig. 9. Simulation results of the MO detection circuits

To assume that a Korean 100 won coin is placed on a detection coil, the simulation is performed by changing the L value to 8.5 μH. In the simulation results, numbers 4 and 5 (the dotted purple and dotted red lines) are the voltages of nodes b and a, respectively, in the presence of the coin. The magnitude of the voltage of node b is reduced to approximately 0.26V, and the magnitude of the voltage of node a is increased to approximately 0.13V. Observing the voltage at node a to determine whether there is a coin or not, a voltage difference

of 0.41 – 0.26 = 0.15V occurs, and a voltage difference of 0.13V occurs when observing the voltage at node b. If the voltage difference between the two nodes is compared, rather than comparing the voltage for only one node, the difference in magnitude is approximately twice.

It is worth noting that the phase difference of the voltage between nodes a and b is approximately 180° when there is a coin. When there is no coin, the maximum value of the voltage product of nodes a and b is less than 0.01. When there is a coin, however, the maximum value is approximately 0.5. That is, when an MO is detected with a change in voltage at one node like the existing detection circuits, the difference is approximately twice. However, as proposed, the difference between the magnitudes of the products of the voltages across the capacitor is approximately 50 times.

The SAE J2954 Standard has physical specifications for wireless charging, but no operation methods. In this paper, a slotted MOD method was used to stop power transmission at regular intervals and detect MOs. In addition, the detection circuit was configured with a resonant circuit for frequency 1 MHz different from power transmission frequency 85 kHz and a resistor to adjust the Q-factor. Therefore, the amount of current induced in the detection coil during power transmission was reduced, and there was no effect from the power transmission signal during MO detection.

3. Implementation and Results

The manufactured PCB MOD coil array and detection circuits are shown in **Fig. 10.a** and **10.b**, respectively. When the inductance of each coil was measured using the measurement equipment, a value similar to the ANSYS Q3D analysis results was measured at approximately 13.4616 μH. When a Korean 100 won coin was placed on the coil, the inductance of the coil was measured as 9.65 μH. In the coil model, it was analyzed as 8.5 μH, but in the actual manufactured coil, the decrease of inductance was less than that of the analysis.

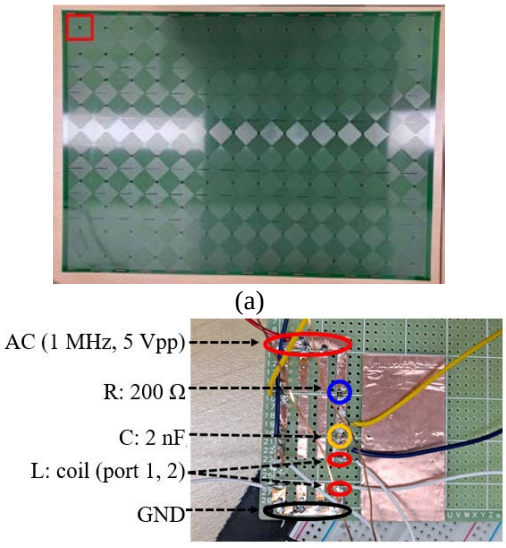

Fig. 10. (a) Manufactured PCB metal object detection coil array (14 x 10) and (b) detection circuits composed of a resistor, a capacitor, and a coil.

The circuit was constructed using a copper plate. From the top, it consists of AC power, a resistor, a capacitor, a coil, and ground. The capacitance of the capacitor was 2nF. AC power was supplied using a Tektronix AFG3021 function generator, and voltage was measured using a Tektronix TBS 1202B-EDU digital oscilloscope.

Fig. 11 shows the oscilloscope when the voltage signals were measured in the absence of MOs. According to the equation $f = 1/\{2\pi\sqrt{LC}\}$, the theoretical resonance frequency is approximately 970 kHz, but the circuit test shows resonance characteristics at approximately 930 kHz. On the oscilloscope's display, the yellow signal (a relatively small signal, unit 50 mV) is the voltage measured at the node between the resistor and the capacitor, and the blue signal (unit 500 mV) is the voltage measured at the node between the capacitor and the coil. The voltage at the node between the resistor and capacitor is approximately 26 mV, and the voltage at the node between the capacitor and coil is measured at approximately 500 mV. There was a phase difference of approximately 90° between the measured voltage signals.

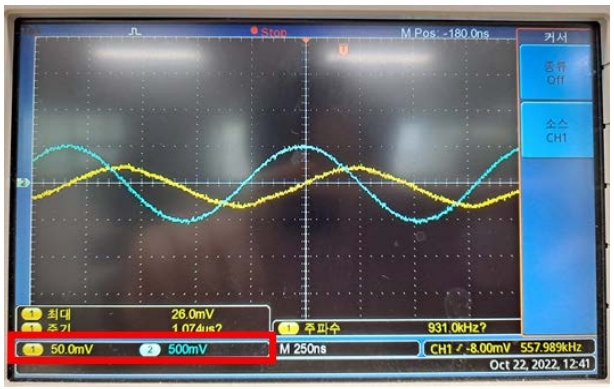

Fig. 11. Voltage signals when there is no MO. Channel 1(yellow line, 50 mV/div): voltage measured at the node between the resistor and the capacitor, and channel 2(blue line, 500 mV/div): voltage measured at the node between the capacitor and the coil.

For the MO detection test, Korean coins of 100 and 500 won were used. A 100 won coin has a diameter of 24 mm and is composed of 75% copper and 25% nickel. A 500 won coin has a diameter of 26.5 mm and is composed of 75% copper and 25% nickel. As shown in **Fig. 12**, the coin was placed at the center of the coil (location 1), edge of the coil (location 2), and boundary of the coil (location 3).

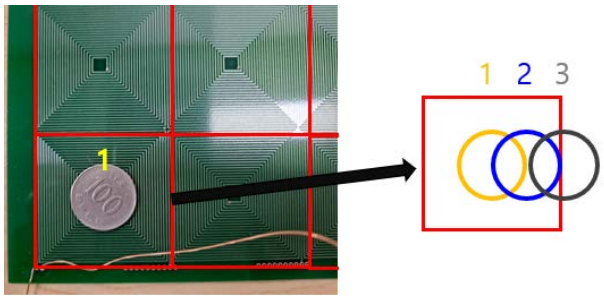

Fig. 12. Environment for MO tests

The results measured with an oscilloscope when a 24 mm diameter 100 won coin is used as the MO are shown in **Fig. 13**. **Fig. 13.a**, **13.b**, and **13.c** show the measured voltage signals when the coin is at locations 1, 2, and 3, respectively. As shown in **Fig. 11**, the yellow signal is the voltage measured at the node between the resistor and capacitor, and the blue signal is

the voltage measured at the node between the capacitor and the coil. When the coin was at location 1, the voltage of the node between the resistor and the capacitor was measured to be approximately 134 mV, and the voltage of the node between the capacitor and the coil was measured to be approximately 400 mV. As a phase difference of approximately 170° was observed between the measured voltage signals. When the coin was in location 2, the voltage of the node between the resistor and the capacitor was measured to be approximately 56 mV, and the voltage of the node between the capacitor and the coil was measured to be approximately 450 mV. A phase difference of approximately 150° was observed between the measured voltage signals. When the coin was in location 3, the voltage of the node between the resistor and the capacitor was measured to be approximately 26 mV, and the voltage of the node between the capacitor and the coil was measured to be approximately 500 mV. A phase difference of approximately 90° was observed between the measured voltage signals.

(a)

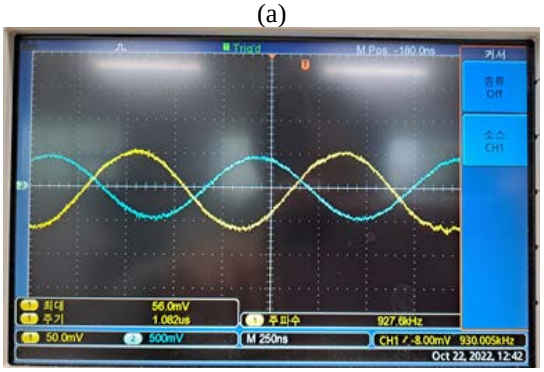

(b)

(c)

Fig. 13. Voltage signals. Channel 1(yellow line, 50 mV/div): voltage measured at the node between the resistor and the capacitor, and channel 2(blue line, 500 mV/div): voltage measured at the node between the capacitor and the coil (a) when the coin is at location 1, (b) location 2, and (c) location 3.

Table 1 summarizes the experimental results for the 24 mm diameter 100 won and 26.5 mm diameter 500 won coins. As in the theoretical analysis, when a coin is placed on the detection coil, the resonance frequency of the circuit, and the magnitude and phase difference of the voltage across the capacitor change. This difference was most evident when the coin was at the center of the coil. The voltage at V_a increased by approximately five times or more, the voltage at V_b decreased to approximately 80%, and the phase difference increased to approximately 170°. The value obtained by multiplying the voltage values of both ends of the capacitor ($|V_a| \times |V_b| \cos\theta$) increased by approximately eight times or more. Therefore, it can be confirmed that the proposed detection circuit is more effective than comparing the values at one node.

Table 1. MO test results. Comparison of voltage, phase and their product according to the location of two MOs

	No coin	**Korean 100 won coin (24 mm in diameter)**			**Korean 500 won coin (26.5 mm in diameter)**		
Location		1	2	3	1	2	3
V_a(mV): V at between R and C	26	134	56	26	160	70	26
V_b (mV): V at between C and L	500	400	450	500	400	475	500
θ (°): Phase difference	90	170	150	90	170	150	90
$(\|V_a\| \times \|V_b\| \cos\theta)$ /1000	6.5	53.6	21.82	6.50	64.00	28.80	6.5

However, the change in impedance of the coil due to the coin became smaller as it moved from the center to the edge of the coil; therefore, when the coin was placed at the boundary of the coil, it had little effect on the coil. This is a problem with the coil arrangement. In the future, by constructing a two-layer coil array and staggering the coil centers of the first and second layers, the blind zone in the first-layer coil array can be improved for detection in the second-layer coil array.

4. Conclusion

In this paper, we proposed circuits that effectively detects metallic foreign objects between the power transmission and reception coils of an electric vehicle wireless charging system. An active detection coil array was used, and 1 MHz AC power was supplied. The characteristic that the impedance of the active detection coil changes when there is a metallic foreign object is used as the basis. Therefore, to represent the voltage change effectively according to the reactance change, capacitors are connected in series to form an LC resonance circuit for a 1 MHz power supply. In general, when using an active detection-only coil, a change in the voltage or current at a specific node of the detection circuit is observed. However, in this study, the presence of metallic foreign objects was determined by multiplying the voltage across the capacitor. When there is no metallic foreign object, the resonance circuit characteristics are exhibited for a 1 MHz power supply. Therefore, the voltage phase difference across the capacitor was 90°, and the voltage magnitude at the node where the capacitor and resistor were connected is approximately zero. However, when a metallic foreign object is inserted, the resonance frequency changes owing to the change in reactance, the voltage phase difference across the capacitor becomes approximately 180°, and the voltage at the node where the capacitor and resistor are connected increases. After making the coil array and detection circuit, the experiment was conducted with Korean 100 won coins 24 mm in diameter. It was confirmed that the product of the voltage at both ends of the capacitor increased by

approximately eight times. This increase is larger than the change of approximately five times when comparing the voltage magnitude at one specific node. Therefore, this detection-only circuit is expected to increase the accuracy of detecting metallic foreign objects in electric vehicle wireless charging systems. However, no change in the voltage was observed when a metallic foreign object was present on the edge of the detection coil. This is due to the structure of the detection coil array and can be solved by configuring the detection coil array in a two-layer structure and staggering the detection and non-detection areas of the first and second layers. In the future, we plan to continue the research on the detection coil array method with a two-layer structure.

References

[1] M. Amjad, M. Farooq-i-Azam, Q. Ni, M. Dong, and E. A. Ansari, “Wireless charging systems for electric vehicles,” *Renewable and Sustainable Energy Reviews*, vol. 167, p. 112730, Oct. 2022. Article (CrossRef Link)

[2] G. Palani, U. Sengamalai, P. Vishnuram, and B. Nastasi, “Challenges and Barriers of Wireless Charging Technologies for Electric Vehicles,” *Energies*, vol. 16, no. 5, p. 2138, 2023. Article (CrossRef Link)

[3] J. M. Miller, O. C. Onar, and M. Chinthavali, "Primary-Side Power Flow Control of Wireless Power Transfer for Electric Vehicle Charging," *IEEE J. Emerg. Sel. Top. Power Electronics*, vol. 3, no. 1, pp. 147-162, March 2015. Article (CrossRef Link)

[4] A. Ahmad, M. S. Alam, and R. Chabaan, "A Comprehensive Review of Wireless Charging Technologies for Electric Vehicles," *IEEE Transactions on Transportation Electrification*, vol. 4, no. 1, pp. 38-63, March 2018. Article (CrossRef Link)

[5] T. U. Chang, Y. S. Ryu, S. K. Song, K. W. Kwon, and J. H. Paik, "Design and Implementation of Distributed Charge Signal Processing Software for Smart Slow and Quick Electric Vehicle Charge," *KSII Transactions on Internet and Information Systems*, vol. 13, no. 3, pp. 1674-1688, 2019. Article (CrossRef Link)

[6] B. A. Rayan, U. Subramaniam, and S. Balamurugan, “Wireless Power Transfer in Electric Vehicles: A Review on Compensation Topologies, Coil Structures, and Safety Aspects,” *Energies*, vol. 16, no. 7, p. 3084, 2023. Article (CrossRef Link)

[7] Wieland Brúch, “Charging even easier than refueling,” BMW Group, May 28, 2018. [Online]. Available: https://www.press.bmwgroup.com/global/article/detail/T0281369EN/charging-even-easier-than-refuelling?language=en.

[8] P. S. Subudhi, and S. Krithiga, "Wireless Power Transfer Topologies used for Static and Dynamic Charging of EV Battery: A Review," *International Journal of Emerging Electric Power Systems*, vol. 21, no. 1, p. 20190151, 2020. Article (CrossRef Link)

[9] S. Son, S. Lee, J. Rhee, Y. Shin, S. Woo, S. Huh, C. Lee, and S. Ahn, "Foreign Object Detection of Wireless Power Transfer System Using Sensor Coil," in *Proc. of 2021 IEEE Wireless Power Transfer Conference (WPTC)*, San Diego, CA, USA, pp. 1-4, 2021. Article (CrossRef Link).

[10] J. Y. Seong, and S.-S. Lee, “Optimization of the Alignment Method for an Electric Vehicle Magnetic Field Wireless Power Transfer System Using a Low-Frequency Ferrite Rod Antenna,” *Energies*, vol. 12, no. 24, p. 4689, 2019. Article (CrossRef Link)

[11] *SAE Recommended Practice J2954 (rev. 201904)*, Society of Automotive Engineers International. Wireless Power Transfer for Light-Duty Plug-In/ Electric Vehicles and Alignment Methodology, Society of Automotive Engineers International: Troy, MI, USA, 2019.

[12] E. Asa, M. Mohammad, O. C. Onar, J. Pries, V. Galigekere, and G. -J. Su, "Review of Safety and Exposure Limits of Electromagnetic Fields (EMF) in Wireless Electric Vehicle Charging (WEVC) Applications," in *Proc. of 2020 IEEE Transportation Electrification Conference & Expo (ITEC)*, Chicago, IL, USA, pp. 17-24, 2020. Article (CrossRef Link).

[13] H. Jiang, P. Brazis, M. Tabaddor, and J. Bablo, "Safety considerations of wireless charger for electric vehicles — A review paper," in *Proc. of 2012 IEEE Symposium on Product Compliance Engineering Proceedings*, Portland, OR, USA, pp. 1-6, 2012. Article (CrossRef Link)
[14] J. Xia, X. Yuan, J. Li, S. Lu, X. Cui, S. Li, and L. M. Fernández-Ramírez, "Foreign Object Detection for Electric Vehicle Wireless Charging," *Electronics*, vol. 9, no. 5, p. 805, May 2020. Article (CrossRef Link)
[15] Y. Tian, W. Guan, G. Li, K. Mehran, J. Tian, and L. Xiang, "A review on foreign object detection for magnetic coupling-based electric vehicle wireless charging," *Green Energy and Intelligent Transportation*, vol. 1, no. 2, pp. 1-14, May, 2022. Article (CrossRef Link)
[16] Y. Zhang, Z. Yan, J. Zhu, S. Li, and C. Mi, "A review of foreign object detection (FOD) for inductive power transfer systems," *eTransportation*, vol. 1, Aug. 2019. Article (CrossRef Link).
[17] Foreign Object Detection System and Method Suitable for Source Resonator of Wireless Energy Transfer System, by P. F. Hoffman, R. J. Boyer, R. A. Henderson. (2016, Apr. 5). US 9,304,042 B2, [Online]. Available: https://patents.google.com/patent/US9304042B2/en.
[18] Y. Tian, Z. Li, Y. Lin, L. Xiang, X. Li, Y. Shao, and J. Tian, "Metal object detection for electric vehicle inductive power transfer systems based on hyperspectral imaging," *Measurement*, vol. 168, 108493, pp. 1-11, 2021. Article (CrossRef Link)
[19] S. Huang, J. Su, S. Dai, C. Tai, and T. Lee, "Enhancement of wireless power transmission with foreign-object detection considerations," in *Proc. of 2017 IEEE 6th Global Conference on Consumer Electronics (GCCE)*, Nagoya, Japan, pp. 1–2, Oct. 2017. Article (CrossRef Link).
[20] L. Xiang, Z. Zhu, J. Tian, and Y. Tian, "Foreign object detection in a wireless power transfer system using symmetrical coil sets," *IEEE Access*, vol. 7, pp. 44622–44631, 2019. Article (CrossRef Link)
[21] V. X. Thai, G. C. Jang, S. Y. Jeong, J. H. Park, Y. -S. Kim, and C. T. Rim, "Symmetric sensing coil design for the blind-zone free metal object detection of a stationary wireless electric vehicles charger," *IEEE Trans. Power Electron.*, vol. 35, no. 4, pp. 3466–3477, Apr. 2020. Article (CrossRef Link)
[22] Foreign object detection in wireless energy transfer systems, by S. Verghese, M.P. Kesler, K.L. Hall, and H.T. Lou (2011, Sep. 9). US 20 130 069 441 A1. [Online]. Available: https://patents.google.com/patent/US20130069441A1/en.
[23] Y. Tian, Y. Lin, J. Tian, and L. Xiang, "Multi-thread sensing coil design for metal object detection of wireless power transfer systems," *Measurement*, vol.184, pp. 1-12, Aug. 2021. Article (CrossRef Link)
[24] S. Kim, H. Jung, Y. Ju, and Y. Lim, "A Novel Metal Foreign Object Detection for Wireless High-Power Transfer Using a Two-Layer Balanced Coil Array with a Serial-Resonance Maxwell Bridge," *Electronics*, vol. 9, no. 12, p. 2070, Dec. 2020. Article (CrossRef Link)
[25] B. Cheng, J. Lu, Y. Zhang, G. Pan, R. Chabaan, and C. C. Mi, "A Metal Object Detection System with Multilayer Detection Coil Layouts for Electric Vehicle Wireless Charging," *energies*, vol. 13, no. 11, p. 2960, June 2020. Article (CrossRef Link)
[26] S. Kim, W. Choi, and Y. Lim, "Metal Object Detection in a Wireless High-Power Transfer System Using Phase–Magnitude Variation," *Electronics*, vol. 10, p. 2952, Nov. 2021. Article (CrossRef Link)

Sunhee Kim received B.S., M.S. and Ph.D degrees in electronic engineering from Ewha Womans University in 2000, 2002, and 2016, respectively. She worked as a researcher in ETRI from 2002 to 2005, and in KETI from 2005 to 2012. Currently, she is an assistant professor at Sangmyung University. Her research interest includes wireless power transfer, wireless communication, and SoCc for them.